Journal of Experimental Botany, Vol. 64, No. 12, pp. 3697–3709, 2013
doi:10.1093/jxb/ert202 Advance Access publication 23 July, 2013
This paper is available online free of all access charges (see http://jxb.oxfordjournals.org/open_access.html for further details)

Journal of Experimental Botany
www.jxb.oxfordjournals.org

RESEARCH PAPER

Emissions of putative isoprene oxidation products from mango branches under abiotic stress

Kolby J. Jardine[1,*], Kimberly Meyers[2], Leif Abrell[3], Eliane G. Alves[4], Ana Maria Yanez Serrano[4,5], Jürgen Kesselmeier[5], Thomas Karl[6], Alex Guenther[6], Jeffrey Q. Chambers[1] and Claudia Vickers[7]

[1] Climate Science Department, Earth Science Division, Lawrence Berkeley National Laboratory, 1 Cyclotron Rd, Building 64, Room 241, Berkeley, CA 94720, USA
[2] US Department of Agriculture, Agriculture Research Service, 2000 East Allen Rd, Tucson, AZ 85719, USA
[3] Department of Chemistry & Biochemistry and Department of Soil, Water and Environmental Science, University of Arizona, PO Box 210038, Tucson, AZ 85721-0038, USA
[4] Large-Scale Biosphere-Atmosphere Experiment (LBA), Instituto Nacional de Pesquisas da Amazônia, Av. André Araújo, 2936, Aleixo, CEP 69060-001, Manaus, Brazil
[5] Biogeochemistry Department, Max Planck Institute for Chemistry, PO Box 3060, 55020 Mainz, Germany
[6] Atmospheric Chemistry Division, National Center for Atmospheric Research, PO Box 3000, Boulder, CO 80307-3000, USA
[7] Australian Institute for Bioengineering and Nanotechnology, The University of Queensland, Building 75, Cnr Cooper and College Rds, St Lucia, QLD 4072, Australia

* To whom correspondence should be addressed. Email: kjjardine@lbl.gov

Received 17 May 2013; Revised 17 May 2013; Accepted 5 June 2013

Abstract

Although several per cent of net carbon assimilation can be re-released as isoprene emissions to the atmosphere by many tropical plants, much uncertainty remains regarding its biological significance. In a previous study, we detected emissions of isoprene and its oxidation products methyl vinyl ketone (MVK) and methacrolein (MACR) from tropical plants under high temperature/light stress, suggesting that isoprene is oxidized not only in the atmosphere but also within plants. However, a comprehensive analysis of the suite of isoprene oxidation products in plants has not been performed and production relationships with environmental stress have not been described. In this study, putative isoprene oxidation products from mango (*Mangifera indica*) branches under abiotic stress were first identified. High temperature/light and freeze–thaw treatments verified direct emissions of the isoprene oxidation products MVK and MACR together with the first observations of 3-methyl furan (3-MF) and 2-methyl-3-buten-2-ol (MBO) as putative novel isoprene oxidation products. Mechanical wounding also stimulated emissions of MVK and MACR. Photosynthesis under $^{13}CO_2$ resulted in rapid (<30 min) labelling of up to five carbon atoms of isoprene, with a similar labelling pattern observed in the putative oxidation products. These observations highlight the need to investigate further the mechanisms of isoprene oxidation within plants under stress and its biological and atmospheric significance.

Keywords: 2-Methyl-3-buten-2-ol, 3-methyl furan, methacrolein, methyl vinyl ketone, reactive oxygen species, volatile organic compounds.

Introduction

Isoprene (C_5H_8) is emitted in large quantities by many terrestrial plants directly into the atmosphere, where it acts to fuel atmospheric chemistry leading to the formation of a number of species with high relevance to air quality and climate

Abbreviations: 3-MF, 3-methyl furan; 3-MT, 3-methyl thiophene; GC-MS, gas chromatography/mass spectrometry; GLV, green leaf volatiles; MACR, methacrolein; MBO, 2-methyl-3-buten-2-ol; MVK, methyl vinyl ketone; NIST, the National Institute of Standards and Technology; PAR, photosynthetically active radiation; PTR-MS, proton transfer reaction/mass spectrometry; ROS, reactive oxygen species; sccm, standard cm3 min–1; slpm, standard l min–1; TD, thermal desorption.

including organic nitrates (Lockwood *et al.*, 2010), ground level ozone (Pierce *et al.*, 1998), and secondary organic aerosols (Kroll *et al.*, 2006) that may act as effective cloud condensation nuclei (Engelhart *et al.*, 2011). Due to its high annual global emission rate of 500–750 Tg year^{-1} (Guenther *et al.*, 2006) and high reactivity to atmospheric oxidants such as the OH radical (Atkinson and Arey, 2003), isoprene emissions from terrestrial vegetation exert a controlling effect on the oxidative power of the lower atmosphere. Once emitted, isoprene is rapidly oxidized in the atmosphere (1–2 h lifetime with respect to oxidation by OH radicals) with first-order oxidation products dominated by formaldehyde (50–70%), methyl vinyl ketone (MVK, 25–39%), methacrolein (MACR, 17–27%), and 3-methyl furan (3-MF, 4.2–5.4%) (Atkinson and Arey, 2003). However, efforts to quantify the magnitude of isoprene chemistry–climate feedbacks have been hindered by major uncertainties as to why plants dedicate a significant fraction (a few per cent under normal physiological conditions) of assimilated carbon to isoprene emissions in the first place (Pacifico *et al.*, 2009). In contrast to its role in atmospheric chemistry, very little is known about the behaviour and effects of isoprene *in planta*, including potential redox reactions and products.

Reactive oxygen species (ROS) including singlet oxygen ($^1O_2$), superoxide anion (O_2^-), hydrogen peroxide (H_2O_2), and the hydroxyl radical (OH) are continuously generated in plants due to the incomplete reduction of oxygen. While initially considered toxic byproducts of aerobic metabolism, ROS are now widely recognized to play a multitude of signalling roles during the regulation of biological processes including growth and development (Foreman *et al.*, 2003), cell cycle (Feher *et al.*, 2008), programmed cell death (Overmyer *et al.*, 2003), hormone signalling and stomatal regulation (Kwak *et al.*, 2003; Pei *et al.*, 2000), and biotic and abiotic stress responses (Mittler, 2002; Mullineaux and Karpinski, 2002). While ROS concentrations within plants are generally kept low by cellular antioxidant defence systems, ROS accumulation during stress can overwhelm these systems, leading to the initiation of defence signalling mechanisms (Miller *et al.*, 2010). A growing body of evidence suggests that isoprene protects plants under stress by functioning as an effective antioxidant (Vickers *et al.*, 2009*a*) and/or by stabilizing membranes (Velikova *et al.*, 2011). Thus, isoprene may protect photosynthesis during stress by stabilizing thylakoid membranes and directly scavenging ROS (Velikova *et al.*, 2012). For example, isoprene increases the plant's ability to conduct photosynthesis at elevated temperatures (Singsaas *et al.*, 1997) and, in the presence of ozone, exogenously supplied isoprene reduces the accumulation of ROS (Loreto *et al.*, 2001; Loreto and Velikova, 2001; Velikova *et al.*, 2004; Vickers *et al.*, 2009*b*).

The isoprene oxidation products MVK and MACR are known to be highly active defence signalling compounds, and can initiate the expression of a wide array of defence genes (Almeras *et al.*, 2003). In line with this, fumigation of plants with MVK resulted in the upregulation of genes involved in defence signalling and ROS metabolism (Karl *et al.*, 2010). This enhanced biological activity derives from the fact that MVK and MACR act as reactive electrophiles due to the presence of α,β-unsaturated carbonyl groups, and therefore show high reactivity with nucleophiles (Uchida *et al.*, 1998). Reactive electrophiles may potentially affect gene expression at all levels by chemically reacting with nucleic acids, proteins, and small molecules as well as by indirectly lowering pools of cellular reductants (Farmer and Davoine, 2007).

Recently, we obtained evidence that isoprene is oxidized not only in the atmosphere but also within plants. Using gas chromatography/mass spectrometry (GC-MS) and proton transfer reaction/mass spectrometry (PTR-MS), we detected gas-phase emissions of isoprene and its oxidation products MVK and MACR from high temperature/light-stressed desert (Jardine *et al.*, 2010*a*) and tropical (Jardine *et al.*, 2012) plants. We demonstrated at the leaf, branch, and enclosed mesocosm scales that higher emissions of MVK+MACR relative to isoprene occurred during high temperature/light stress. In addition, leaf feeding of pyruvate-2-^{13}C (a precursur of isoprene) through the transpiration stream was used to track ^{13}C into *de novo* isoprene biosynthesis and its oxidation products MVK and MACR, suggesting that these compounds are produced directly from isoprene reactions.

In this study, using a coupled PTR-MS, GC-MS, and photosynthesis system, we first investigated branch-level emissions of isoprene and putative isoprene oxidation products MVK and MACR from a high isoprene-emitting species, *Mangifera indica* (mango), and a non-isoprene-emitting species *Annona muricata* (soursop) under abiotic stress including high temperature/light, freeze–thaw/dehydration, and mechanical wounding. Next, we quantified emissions of the putative novel isoprene oxidation products 3-MF, 3-methyl thiophene (3-MT), and 2-methyl-3-buten-2-ol (MBO) from mango branches in response to abiotic stress. Finally, we explored the possibility that these compounds derive from isoprene oxidation within plants (Fig. 1) by tracking isoprene biosynthesis and volatile emissions during photosynthesis under $^{13}CO_2$.

Materials and methods

Experimental setup

A recent synthesis paper on isoprene emissions from terrestrial ecosystems found that only three out of 20 publications reviewed reported isoprene emissions from tropical regions, even though the tropics were estimated to contribute ~80% of global annual isoprene emissions (Guenther *et al.*, 2006). Previous studies (Harley *et al.*, 2004; Jardine *et al.*, 2010*b*, 2012) found high isoprene emissions from leaves of tropical mango trees (*Mangifera indica*). We therefore used mango as a representative tropical species from which to study isoprene biosynthesis, oxidation, and emission. For this purpose, a single mango tree (~7 m tall) and soursop tree (*Annona muricata*, a non-isoprene emitter, ~5 m tall) located inside the large environmentally controlled mesocosm at Biosphere 2 (Allen *et al.*, 2003) were used for the branch enclosure experiments. In addition, three potted (~1 m tall) mango trees (Top Tropicals), grown under controlled growth conditions at Lawrence Berkeley National Laboratory, USA were also used to evaluate the relationship between leaf temperature, net photosynthesis, stomatal conductance to water vapour, and isoprene emissions using a LI-6400XT photosynthesis system (LI-COR Biosciences).

Measurements of leaf isoprene emissions (one leaf on each of the three potted plants) in relation to plant physiological variables was made by modifying the LI-6400XT such that 100 standard cm^3 min^{-1}

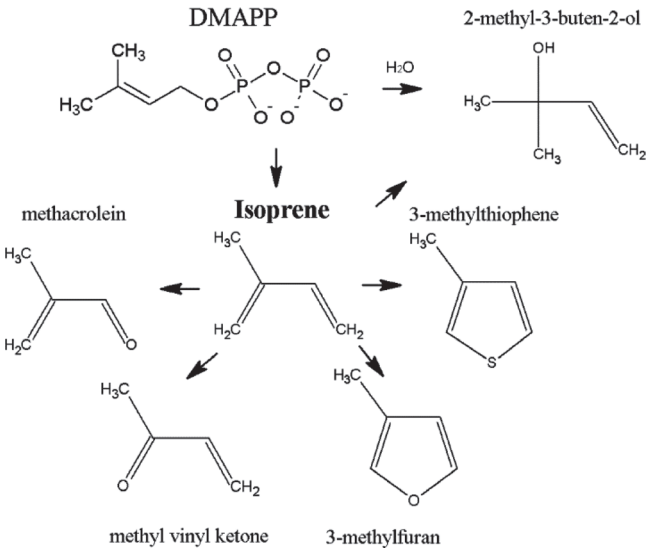

Fig. 1. Diagram of isoprene and its potential oxidation products. Isoprene is first synthesized from dimethylallyl diphosphate (DMAPP,) which might also form MBO if water is allowed to enter the active site of isoprene synthase (Gray *et al.*, 2011). Isoprene may then be oxidized to MACR, MVK, 3-MF, 3-MT, and MBO via enzymatic and/or non-enzymatic mechanisms.

(sccm) of the flow out of the leaf chamber was diverted to a thermal desorption tube for analysis by GC-MS, as described previously (Harley *et al.*, 2004). Branch emissions of isoprene and its putative oxidation products were identified and quantified using a coupled GC-MS, PTR-MS, and photosynthesis system as described below. Stems of individual detached branches were placed in tap water after removal from the tree and immediately re-cut under water before being transported to the laboratory where they were placed inside a ~4.0 l Teflon branch enclosure with 3.0 standard l min^{-1} (slpm) of hydrocarbon-free air flowing through. CO_2 concentrations entering the enclosure were adjusted to 400–800 ppmv by diluting 1.2–2.4 sccm pure CO_2 with 3.0 slpm of hydrocarbon-free air.

Gas samples inside the branch enclosure were continuously drawn through a 1/4 inch outer-diameter Teflon tube connected to a four way union that was diverted to an infrared gas analyser (~500 sccm, LI-7000; LI-COR Biosciences), a high-sensitivity PTR-MS (~50 sccm), and a thermal desorption GC-MS (~200 sccm when sampling). The excess flow not diverted for analysis was vented to the room where the enclosure was fixed to the branch (Supplementary Fig. S1 at *JXB* online). A three-way valve (Teflon PTFE; Cole-Parmer) was installed upstream of the tee to allow the analysis of either air entering the enclosure or air inside the enclosure. To aid in compound identification, during initial experiments on two detached mango branches, the hydrocarbon-free airflow entering the enclosure was reduced to 1.0 slpm to increase concentrations of all compounds of interest inside the branch enclosure. All flow rates were controlled with mass flow controllers (Cole-Parmer). Light was supplied to the branch with an LED grow light (600 W; AIBC International), which generated photosynthetically active radiation (PAR) intensities at the top branch height of between 275 and 640 µmol m^{-2} s^{-1}, depending on the height of the branch. Enclosure air temperatures ranged from 19 to 25 °C. Enclosure air temperatures and PAR were measured using a quantum light sensor (placed at branch height) and a temperature microsensor (placed inside the enclosure in the shaded region under a leaf), respectively and stored every 5 min on a watchdog data logger (Spectrum Technologies).

Two separate thermal desorption (TD) tubes were run sequentially on the GC-MS system (see description below) without sample collection in order to clean the tubes for subsequent trace analysis. Following this, background samples (enclosure blanks) for each of the two TD tubes were collected from an empty enclosure in the light in parallel with PTR-MS and LI-7000 measurements prior to introduction of the branch. This procedure resulted in clean GC-MS backgrounds with negligible concentrations of the volatiles of interest observed in the empty enclosure (<0.02 ppbv). To prevent room air from being measured while the branch was being installed, the three-way valve was switched to the position that diverted a portion of the air entering the enclosure to the PTR-MS and LI-7000. After 5–10 min following the installation of the branch in the enclosure, the three-way valve was switched such that air inside the enclosure was analysed. PTR-MS and LI-7000 trace gas measurements continued in real-time while samples were collected on the TD tubes manually for 30 min and immediately run on the GC-MS. The second TD tube was attached for sample collection immediately after the first TD tube was detached for analysis so that consecutive samples were taken.

^{13}C-labelling experiments

Carbon used for isoprene biosynthesis is strongly linked with photosynthesis under unstressed conditions (Karl *et al.*, 2002). We therefore measured the incorporation of ^{13}C into volatile emissions under $^{13}CO_2$. These experiments were designed to help determine whether the putative isoprene oxidation products were indeed associated with the rapid *de novo* biosynthesis of isoprene without artificially altering precursor substrate pools (e.g. pyruvate). During ^{13}C-labelling experiments, 99% $^{13}CO_2$ (Cambridge Isotope Laboratories) was introduced at a flow rate of 1.3–3.0 sccm into 3.0 slpm hydrocarbon-free airflow entering the enclosure to generate $^{13}CO_2$ concentrations between 429 and 989 ppmv. Following introduction of the mango branch into the enclosure, four to six TD samples were collected and analysed by GC-MS in parallel with online PTR-MS and LI-7000 measurements. Although the LI-7000 has reduced sensitivity to $^{13}CO_2$ relative to $^{12}CO_2$ (~10%), net assimilation of $^{13}CO_2$ during photosynthesis could still be monitored. Real-time labelling patterns of isoprene were monitored using PTR-MS signals at mass-to-charge ratios (*m*/*z*) of 69–74, which represent ^{13}C-labelling of between zero and five carbon atoms, respectively (Karl *et al.*, 2002). Significant PTR-MS interferences between ^{13}C-labelled isoprene and its ^{13}C-labelled oxidation products occurred (e.g. the ^{13}C-labelled isoprene range of *m*/*z* 69–74 strongly overlapped the ^{13}C-labelled MVK+MACR range of *m*/*z* 71–75). Therefore, we used GC-MS mass spectra of isoprene and its putative oxidation products for ^{13}C-labelling analysis. For GC-MS analysis, relative ion intensities over the mass range corresponding to the parent ion and the fully ^{13}C-labelled ion were also determined. As the parent ion of MBO is not present in significant amounts due to extensive fragmentation during electron impact ionization in the GC-MS, we used a major four-carbon fragment at *m*/*z* 71 for ^{13}C-labelling analysis of MBO. Thus, relative mass spectra were determined for isoprene (*m*/*z* 68–73), MBO (*m*/*z* 71–75), MVK and MACR (*m*/*z* 70–74), 3-MF (*m*/*z* 82–87), and 3-MT (*m*/*z* 98–103). The experiment was repeated on three different mango branches.

Abiotic stress treatments

Abiotic stress experiments in the laboratory were performed on detached branches and included high light/temperature, freeze–thaw/desiccation, and mechanical wounding stress. High temperature/light stress experiments (five mango branches and three soursop branches) were performed under air (3.0 l min^{-1} dry hydrocarbon-free air flowing into the enclosure). After the branch was allowed to stabilize inside the enclosure for ~1 h (two TD tube samples collected), the lamp used to illuminate the chamber was lowered until PAR intensities at branch height increased from 275–640 to 2000–2500 µmol m^{-2} s^{-1} and enclosure air temperatures increased from 19–25 to 35–45 °C. Following the lowering of the grow lamp, four TD tube samples were collected and analysed by GC-MS in parallel with

online PTR-MS and LI-7000 measurements. During freeze–thaw/desiccation experiments (three mango branches and three soursop branches), detached branches were first placed in a freezer overnight (–18 °C) before being placed in the branch enclosure under normal PAR and air temperature conditions. Prior to inserting the branch in the enclosure, the stem was placed in tap water without recutting the stem. Once in the enclosure, five to ten TD tube samples of enclosure air were collected and analysed by GC-MS in parallel with online PTR-MS and LI-7000 measurements. Abiotic stress experiments in the laboratory were also performed on detached branches following mechanical wounding (three mango branches and three soursop branches). After installing the branch in the enclosure under normal PAR and air temperature conditions (275–640 µmol m^{-2} s^{-1}, 19–25°C), two TD tube samples were collected and analysed by GC-MS in parallel with online PTR-MS and LI-7000 measurements. Following this, the three-way valve was activated to allow air entering the enclosure to be analysed by the PTR-MS and LI-7000 while the branch enclosure was opened and each leaf on the branch was cut with scissors three times (~5 cm per cut with a typical leaf length of 25 cm). After reclosing the enclosure and waiting 5 min for any room air to be flushed out, the three-way valve was deactivated and three TD tube samples were collected sequentially and analysed by GC-MS in parallel with online PTR-MS and LI-7000 measurements.

TD GC-MS

Enclosure air samples (6.0 l) were collected by drawing enclosure air through one of two TD tubes for 30 min at a flow rate of 200 sccm. Sample airflow rate was regulated by a mass flow controller and a pump downstream of the TD tube. Each of the two TD tubes was filled with Tenax TA, graphitized carbon, and Carboxen 1000 adsorbents (Markes International). These adsorbents were selected in order to minimize water vapour collection and to quantitatively collect pptv to ppbv levels of C_4–C_5 volatiles on the graphitized carbon and Carboxen 1000 adsorbents. The Tenax TA adsorbent reversibly bound higher-molecular-weight compounds (e.g. C_{15}–C_{18}), which prevented their irreversible binding to the stronger graphitized carbon and Carboxen 1000 adsorbents. Immediately following sample collection, the TD tube sample was analysed utilizing a UNITY 2 thermal desorption system (Markes International), which was directly connected to a 5975C series gas chromatograph/electron impact mass spectrometer with a triple-axis detector (Agilent Technologies). After loading a TD tube in the UNITY 2 thermal desorption system, the collected samples were dried for 3 min with 30 sccm of ultra-high purity helium (all flow vented out of the split vent) before being heated to 300 °C for 5 min with 50 sccm of helium and transferred to the UNITY 2 cold trap (water management cold trap; Markes International) held at 30 °C. During injection, the trap was heated to 300 °C for 3 min while back-flushing with carrier gas at a flow of 6.5 sccm. To improve peak shape and further reduce the amount of water introduced into the GC-MS, 5 sccm of this flow was vented through the split while the remaining 1.5 sccm was directed to the column (60 m×0.32 mm×1.8 µm, D-B624; Agilent), temperature programmed with an initial hold of 3 min at 40 °C followed by an increase to 220 °C at 6 °C min^{-1} followed by a hold at 220 °C for 1 min. The mass spectrometer was configured for trace analysis with a 15× detector gain factor and scan mode (*m/z* 40–120). Calibration of the GC-MS to isoprene (1.0 mM), MACR (1.2 mM), MVK (1.2 mM), 3-MF (1.1 mM), MBO (1.0 mM), and 3-MT (1.0 mM) was accomplished using the dynamic solution injection technique (Jardine *et al.*, 2010*c*) with a methanol solution (Sigma-Aldrich). Gas-phase concentrations (10.7–13.8 ppbv) of target analytes were generated using a liquid injection flow rate of 0.5 µl min^{-1} continuously evaporated into a 1.0 l min^{-1} flow of zero air. After analysing a blank TD tube without sample collection, the calibration gas was collected and analysed (calibration air sample collected on the same TD tube for 5 min at 200 ml min^{-1}). Identification of target analytes in enclosure air was confirmed by comparison of mass spectra with the National Institute of Standards and Technology (NIST) mass spectral library and the standard, and by comparison of retention times. Target analytes were quantified in sample air by multiplying the peak area of the target ion (isoprene, *m/z* 68; MACR, *m/z* 70; MVK, *m/z* 70; 3-MF, *m/z* 82; MBO, *m/z* 71; 3-MT, *m/z* 97) by the calibration slope.

PTR-MS

The target volatiles were analysed from the enclosure and ambient air samples using a high-sensitivity PTR-MS (IONICON, Austria). The PTR-MS, which is based on quadrupole mass spectrometry (Lindinger and Hansel, 1997), was operated under standard conditions with a drift tube voltage of 600 V and drift tube pressure of 2.0 mb. The following *m/z* values were monitored during each PTR-MS measurement cycle; 21 ($H_3{}^{18}O^+$), 32 ($O_2{}^+$), and 37 (H_2O–H_3O^+), with a dwell time of 20 ms each. The following *m/z* values were also measured sequentially and corresponded to the protonated molecular weights (parent ions), with a 2 s dwell time: *m/z* 69 (isoprene), *m/z* 71 (MVK+MACR), *m/z* 83 [3-MF+C_6 green leaf volatiles (GLVs)], *m/z* 87 (MBO+C_5 green leaf volatiles), and *m/z* 99 (3-MF+C_6 GLVs). The PTR-MS was calibrated using the same dynamic liquid injection method as described previously for GC-MS but with the use of cyclohexane as the solvent. A cyclohexane solution was prepared by dissolving 20 µl each of isoprene, MVK, MACR, MBO, and 3-MT liquid standards (Sigma-Aldrich) in 100 ml of cyclohexane. 3-MF was not added to the solution due to formation of precipitates upon addition to the solvent. Therefore, the calibration slope of 3-MF was assumed identical to that of 3-MT.

Although good quantitative agreement was obtained between GC-MS and PTR-MS concentration measurements of MVK and MACR in mango enclosures (total MVK+MACR concentrations measured by PTR-MS), those for MBO, 3-MF, and 3-MT were overestimated by PTR-MS relative to GC-MS. GC-MS chromatograms revealed that this was probably due to the emissions of C_5 and C_6 GLVs, which are known to be released from plants under stress and probably interfere with PTR-MS signals at *m/z* 87 (MBO+C5 GLVs), *m/z* 83 (3-MF+C6 GLVs), and *m/z* 99 (3-MT+C6 GLVs) (Fall *et al.*, 1999, 2001). For example, abiotic stress treatments induced the emissions of C_5 GLVs (e.g. 3-pentanone, 3-penten-2-ol, 2-penten-1-ol, 2-pentene, 2-penten-3-ol, 1-pentanol, 4-penten-1-ol) and C_6 GLVs (e.g. 3-hexenal, 3-hexen-1-ol, 3-hexen-1-yl acetate) identified only from mass spectra comparison with the NIST mass spectral library (and not quantified). Therefore, we used GC-MS to quantify enclosure concentrations of MBO, 3-MF, and 3-MT.

Results

Identification of putative isoprene oxidation product emissions from mango branches

Detached branches of mango were studied with the intent of identifying primary emissions of putative isoprene oxidation products. In order to increase the enclosure concentrations to aid in compound identification of volatile species in the initial experiments, a low flow rate of hydrocarbon-free air (1.0 l min^{-1}) was introduced into the ~4 l branch enclosure. Fig. 2 shows an example GC-MS chromatogram from headspace samples with isoprene [retention time (RT): 7.00 min, 301.6 ppbv] and five putative oxidation products including MACR (RT: 9.58 min, 5.9 ppbv), MVK (RT: 10.45 min, 6.1 ppbv), 3-MF (RT: 10.59 min, 6.2 ppbv), MBO (RT: 11.39 min, 2.5 ppbv), and 3-MT (RT: 16.93 min, 6.7 ppbv). When the experiment was repeated with a different mango branch, high concentrations of all putative isoprene oxidation products except

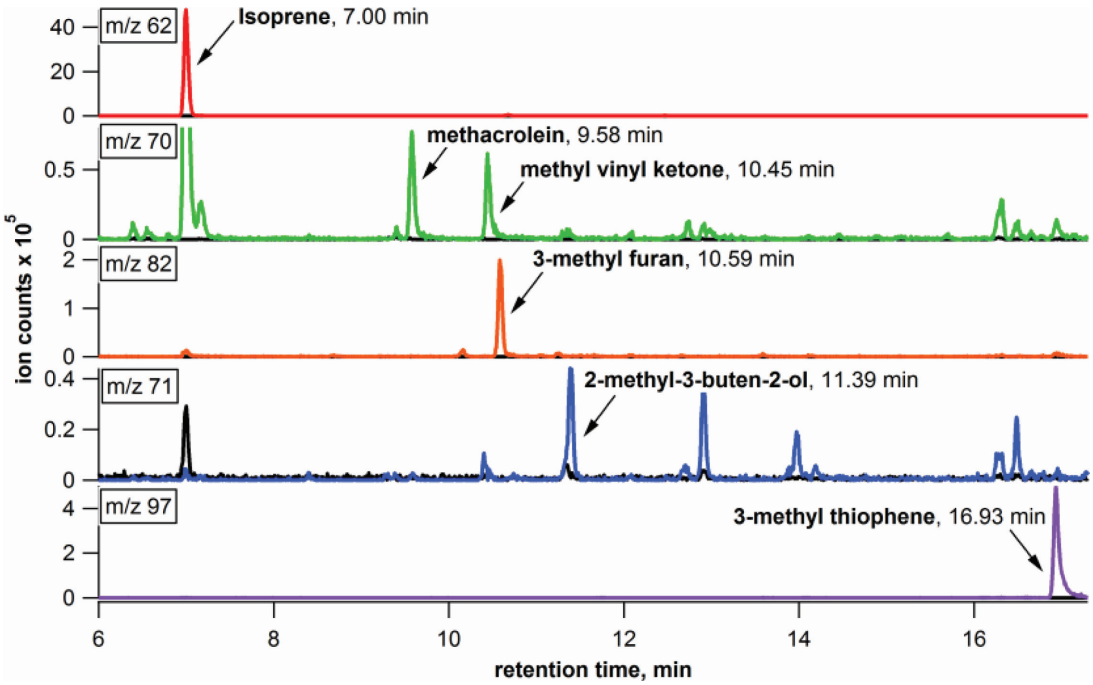

Fig. 2. Single-ion GC-MS chromatogram of an air sample collected from the headspace of a detached mango branch inside a dynamic branch enclosure. Also plotted in black is a control chromatogram of an air sample collected from the enclosure without a branch. The results show the presence of isoprene and five of its putative oxidation products as direct emissions.

3-MT were observed (MACR, 13.6 ppbv; MVK, 15.5 ppbv; 3-MF, 4.1 ppbv; MBO, 84.5; 3-MT, 0.1 ppbv). An analysis of enclosure blanks under identical conditions but without a mango branch revealed low background concentrations of these compounds (<0.2 ppbv). The identification of these putative isoprene oxidation products emitted from mango branches was verified by GC-MS with authentic standards by comparison of retention times and mass spectra. Although the possibility exists that the oxidized volatiles observed arose from isoprene oxidation in the enclosure following isoprene emissions rather than from a reaction *in planta*, it is very unlikely. While gas-phase oxidant concentrations (e.g. ozone) were not measured in the branch enclosure, their role in gas-phase isoprene oxidation was considered negligible due to the use of a high-purity hydrocarbon-free air generator with an ozone output rated less than 1 ppbv (737 Pure Air Generator; AADCO Instruments). In addition, ozone production within the enclosure itself was prevented through the use of a light source without UV light output (600 W LED grow light output wavelengths: red, 630–660 nm; blue, 460 nm; orange, 612 nm; AIBC International). Finally, the residence time in the enclosure was short, in the order of a few minutes.

$^{13}CO_2$-labelling experiments

In order to examine further the possible role of isoprene oxidation within mango leaves as a within-leaf source of MVK, MACR, MBO, 3-MF, and 3-MT emissions, $^{13}CO_2$ labelling was performed on detached mango branches inside the laboratory under controlled lighting conditions. During these experiments, continuous measurements of $^{13}CO_2$ and volatile emissions using online LI-7000 and PTR-MS and near real-time GC-MS were made. While the LI-7000 has greatly reduced sensitivity to $^{13}CO_2$ relative to $^{12}CO_2$, net assimilation of $^{13}CO_2$ during photosynthesis could still be monitored by comparing the measured signal from air with known $^{13}CO_2$ entering the branch enclosure with that of air inside the enclosure. For example, upon placing the branch in the enclosure with ~500 ppmv $^{13}CO_2$ flowing in, the $^{13}CO_2$ enclosure concentrations decreased reaching a minimum after ~30 min (Fig. 3, top panel) and then increased over the remainder of the experiment to the levels of the incoming $^{13}CO_2$ concentrations. Online PTR-MS observations of branch enclosure air showed that photosynthesis under $^{13}CO_2$ led to the rapid ^{13}C-labelling of isoprene emissions (Fig. 3, top panel), as observed previously (Karl *et al.*, 2002; Vickers *et al.*, 2011). However, while the total isoprene concentration increased until peaking after ~30 min, it then declined over the remainder of the experiment. A decline in overall isoprene emission levels over time after the original peak was a common feature of all detached mango branches studied; we presumed that this was due to declines in photosynthesis, as $^{13}CO_2$ concentrations in the enclosure (a proxy for photoassimilation) were inversely correlated with total isoprene emissions. Loss of photosynthetic capacity and isoprene emissions may be a stress response to severing the branch and placing it inside the enclosure.

Upon initially placing the mango branch shown in Fig. 3 in the enclosure (10:27 a.m.), emissions of fully unlabelled isoprene (*m/z* 69) dominated. However, within 3 min of replacing $^{12}CO_2$ with $^{13}CO_2$ (10:30 a.m.), emissions of all ^{13}C-labelled isotopologues increased while emissions of the fully unlabelled isotopologue began to decline. After 25 min

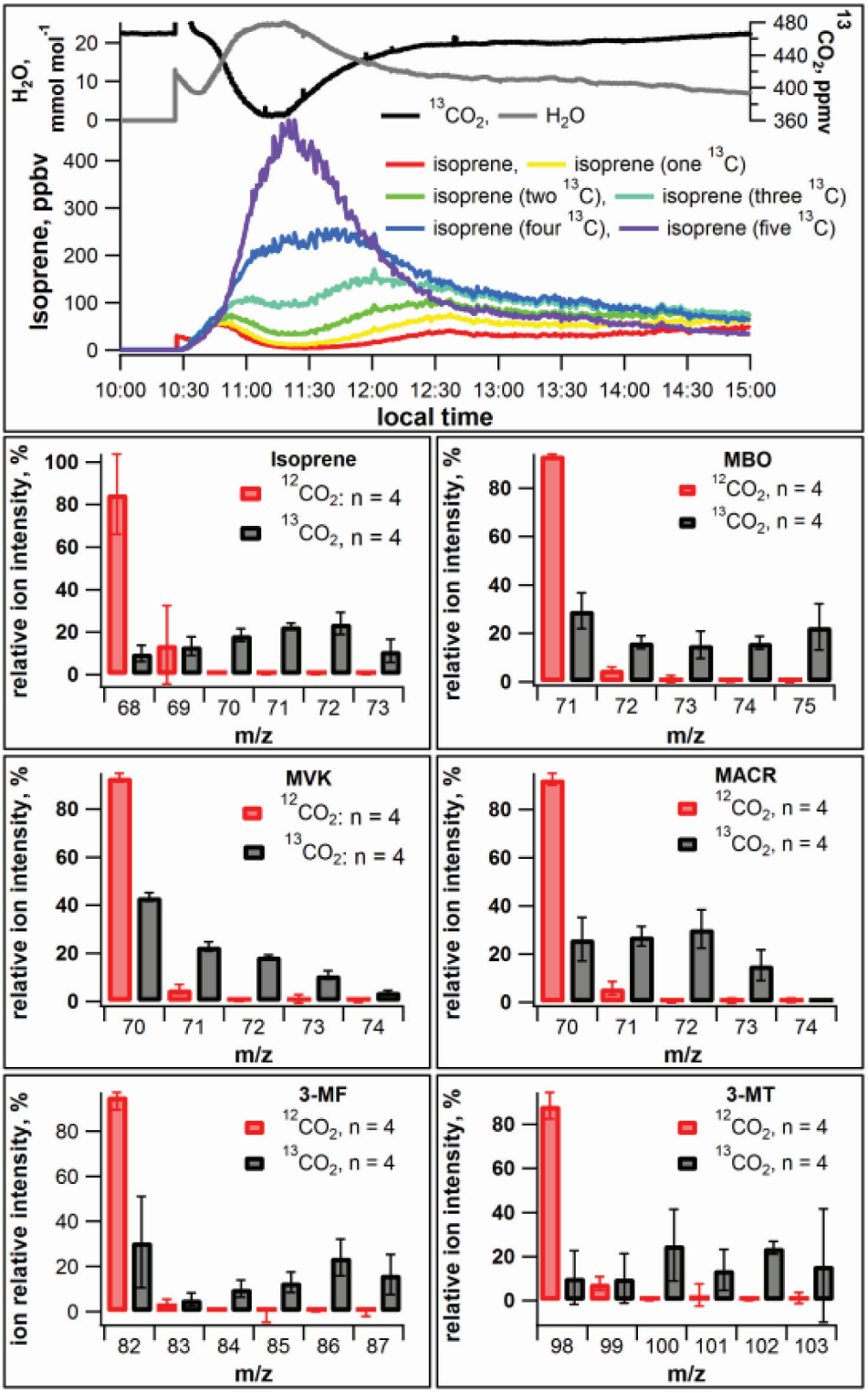

Fig. 3. PTR-MS time series plot showing isoprene ^{13}C-labelling dynamics under $^{13}CO_2$ (top panel) and GC-MS relative ion intensities of isoprene and its five putative oxidation products from a mango branch during photosynthesis under $^{12}CO_2$ and $^{13}CO_2$ (lower panels). The branch was placed in the empty enclosure at 10.27 a.m. and isoprene isotopologue concentrations were monitored by PTR-MS while four sequential TD tubes were collected for GC-MS analysis. The ^{13}C-labelling pattern of isoprene followed $^{13}CO_2$ assimilation, which initially increased and then decreased as the stomata opened and closed (typical response of detached mango branches). Note that, relative to assimilation under natural abundance CO_2 ($^{12}CO_2$), strong ^{13}C labelling was observed in isoprene and its five putative oxidation products.

of photosynthesis under $^{13}CO_2$ (10:52 a.m.), emissions of the fully ^{13}C-labelled isoprene isotopologue (*m*/*z* 74) dominated emissions. During this period, photosynthesis was also increasing and reached a maximum after 53 min (11:20 a.m.), the same approximate time that emissions of the fully labelled isotopologue of isoprene (*m*/*z* 74) peaked and emissions of the unlabelled isotopologue of isoprene (*m*/*z* 69) reached a minimum. This was followed by a decline in net photosynthesis and emissions of fully labelled isoprene (*m*/*z* 74) and a corresponding increase in unlabelled isoprene emissions (*m*/*z* 69). Thus, the temporal dynamics of fully unlabelled isoprene emissions (*m*/*z* 69) and the fully labelled isoprene emissions (*m*/*z* 74) were anti-correlated as the ^{13}C content of the isoprene precursor pools filled and then declined. The increase in unlabelled isoprene after the peak in emissions indicated a carbon source switch for isoprene, with photosynthesis dominating during the first part and an increased contribution from non-photosynthetic sources (e.g. glycolysis) during the decline of photosynthesis. Similar switches in carbon source usage have been observed previously in plants under stress (Loreto and Delfine, 2000; Funk *et al.*, 2004).

Due to the acquisition of multiple ^{13}C atoms during $^{13}CO_2$-labelling experiments, extensive overlap between the PTR-MS signals corresponding to the labelled isotopologues of isoprene and its putative oxidation products exists (e.g. isoprene *m*/*z* 69–74 and MVK+MACR *m*/*z* 71–75). Therefore, we relied on GC-MS analysis of the enclosure air to assess the ^{13}C-labelling pattern of putative isoprene oxidation products with a total concentration estimated to be less than 5–10 ppbv. Thus, isoprene oxidation products accounted for only a few per cent of PTR-MS signals for isoprene isotopologues. GC-MS analysis of enclosure air during the ^{13}C-labelling experiment (four enclosure air samples sequentially collected and analysed) revealed that, relative to emissions under natural abundance CO_2 (four enclosure air samples sequentially collected and analysed from a separate mango branch under $^{12}CO_2$), a strong ^{13}C-labelling pattern was observed for both isoprene and its five putative oxidation products, with all carbon atoms acquiring a ^{13}C atom in most cases (average relative ion abundances across the four GC-MS samples for each shown in Fig. 3, lower panels). Note that, for isoprene, the GC-MS relative mass spectra indicated labelling of all five carbon atoms. However, ^{13}C labelling of the *m*/*z* 67 fragment ion interfered with the ^{13}C-labelling pattern of the molecular ion (*m*/*z* 68), resulting in the dominance of the *m*/*z* 72 ion rather than the *m*/*z* 73 ion. Nevertheless, a similar ^{13}C-labelling pattern observed for isoprene by PTR-MS was also observed by GC-MS.

Abiotic stress

In order to investigate further the hypothesis that the five oxidized volatiles (MVK, MACR, 3-MF, 3-MT, and MBO) derived from the oxidation of isoprene within plants, we conducted a series of abiotic stress treatments known to induce oxidative damage in plants. These experiments included high light/temperature stress, freeze–thaw stress, and mechanical wounding stress.

Upon placing the detached mango branches in the enclosure with 3.0 slpm of hydrocarbon-free air flowing through and normal temperature/light conditions, slightly elevated enclosure concentrations of the putative isoprene oxidation products were observed. However, upon induction of high temperature/light stress, the emission rates increased with elevated concentrations of 3-MF (0.3–3.7 ppbv), MACR, (2.1–6.8 ppbv), MBO (0.7–2.4 ppbv), and MVK (0.4–0.6 ppbv) (Fig. 4a). Only a trace amount of 3-MT could be detected following the heat stress (0.02–0.16 ppbv); levels remained very low and no clear pattern could be observed. For the mango branch shown in Fig. 4, which was monitored for 4.5 h following the application of high temperature/light stress, MVK increased transiently (concentrations doubled to 0.4 ppbv) and then plateaued and sharply declined towards the end of the experiment to low levels (0.02 ppbv). The MBO enclosure concentrations followed a similar pattern but with a higher magnitude. peaking relatively rapidly following the stress (concentrations slightly more than doubled to 0.9 ppbv), plateauing and then declining slightly towards the end of the experiment (0.6 ppbv). 3-MF enclosure concentrations peaked more slowly, increasing to a maximum of 3.7 ppbv, approximately 18.5-fold higher than before the stress. However, similar to MVK concentrations, a sharp decline was observed towards the end of the experiment such that concentrations were very low by the end of the experiment (0.01 ppbv). In contrast, MACR concentrations showed a very different pattern. Upon application of the high temperature/light stress, MACR concentrations increased gradually in the enclosure over time, reaching 2.1 ppbv at the end of the experiment (13-fold increase) and displayed an inverse pattern to isoprene concentrations. To investigate further the possible connections between the proposed isoprene oxidation products and the isoprene emissions of the mango plants, the non-isoprene-emitting tropical plant soursop was utilized as a control. The same high temperature/light stress experiments under air were performed following the same procedure as was used for the mango branches. As shown in Fig. 4b, enhanced emissions of the putative isoprene oxidation products were not observed from soursop branches following high temperature/light stress (enclosure concentrations <0.2 ppbv). Due to issues in branch enclosures including shading, variations in total leaf area, and different leaf temperatures, we utilized a leaf photosynthesis system (LI-6400XT) to evaluate the relationship between leaf temperature, stomatal conductance to water vapour, and isoprene emissions from mango leaves (Fig. 5). Similar to previous leaf level studies on mango leaves (Harley *et al.*, 2004), the maximum temperature for isoprene emissions (37.5 °C) was higher than that of the maximum temperature for photosynthesis and stomatal conductance (32 °C).

Of all of the abiotic stress treatments, branch freeze–thaw/desiccation treatment resulted in the highest enclosure concentrations of the MACR and MVK products (Fig. 6, left panel). However, levels of 3-MF and MBO were similar to those seen in the high-temperature/light-stress experiment, and 3-MT remained low (<0.2 ppbv) during these experiments. For example, during the freeze-thaw/desiccation experiment

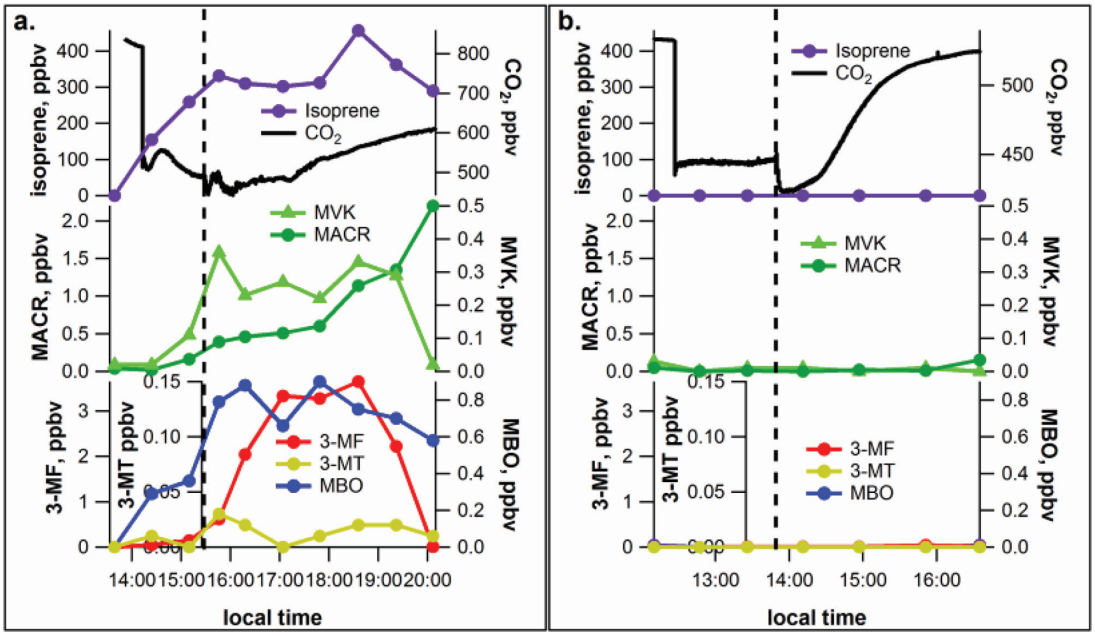

Fig. 4. Example time series plot showing mango (a) and soursop (b) branch enclosure concentrations of isoprene and its five putative isoprene oxidation products, MVK, MACR, 3-MF, MBO, and 3-MT, following high-temperature/light stress. The vertical dashed line represents the time at which the stress was applied. The first GC-MS sample was collected from an empty enclosure just prior to placing the mango branch inside.

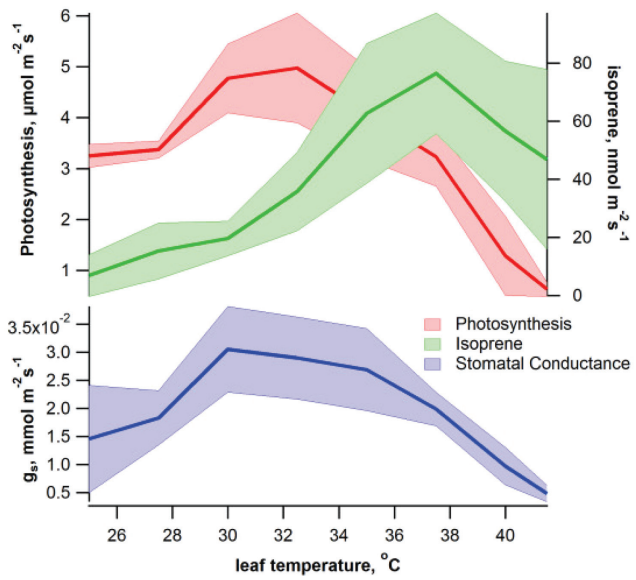

Fig. 5. Plot showing dependencies of net photosynthesis, stomatal conductance to water vapour, and isoprene emission rates on leaf temperature. The shaded areas represent the range from three mango leaves (mean ±1 standard deviation).

shown in Fig. 6, MACR concentrations within the enclosure were 0.0 ppbv when the frozen branch was initially placed into the enclosure, and increased to 16.7 ppbv after 5 h. 3-MF concentrations peaked early, reaching 3.3 ppbv within 38 min and then declined sharply after they peaked and remained low (<0.2 ppbv) for the remainder of the experiment. MVK and MBO concentrations both increased more slowly, reaching peaks of 3.0 and 0.6 ppbv, respectively, after 70 min and declined thereafter. Net photosynthesis was recorded as zero during the thawing process; consequently, isoprene concentrations in the enclosure were low. For example, in the branch shown in Fig. 6, isoprene concentrations peaked at 5.9 ppbv and declined to 1.3 ppbv after 5 h. Isoprene emission levels were essentially inversely correlated with MACR levels, similar to the high-temperature/light-stress experiment shown in Fig. 4. During identical branch freeze–thaw experiments with the non-isoprene-emitting plant soursop, concentrations of the putative isoprene oxidation products remained less than 0.2 ppbv (Fig. 6b).

The final abiotic stress utilized for potential stimulation of isoprene oxidation product emissions involved mechanical leaf wounding. During these experiments, elevated enclosure concentrations of MACR and MVK were observed from two out of three mango branches investigated in response to the leaf wounding (Fig. 7a). However, elevated concentrations of MBO, 3-MF, and 3-MT were not observed. MACR levels showed a small increase after wounding (0.3–0.6 ppbv) and declined thereafter. MVK emissions showed a higher increase after wounding (0.8–0.9 ppbv), also declining thereafter. Identical leaf-cutting experiments on soursop leaves did not lead to elevated enclosure concentrations of MACR and MVK (Fig. 7b).

Discussion

In this study, we verified previous observations that isoprene emissions become uncoupled from photosynthesis (Keller and Lerdau, 1999) and stomatal conductance (Fall and

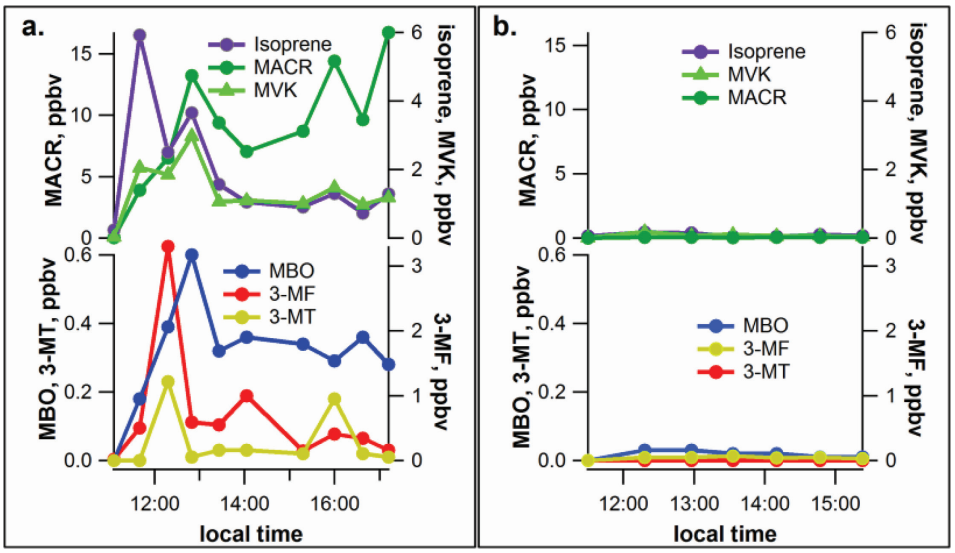

Fig. 6. Example GC-MS time series plot showing increases in branch enclosure concentrations of potential isoprene oxidation products MACR, MVK, MBO, 3-MF, and 3-MT from a mango branch (a) and soursop branch (b) during thawing following a freezing treatment. The first data point is a background sample without a branch inside the enclosure. Note the strong emissions of MACR towards the end of the experiment. The freeze–thaw treatment prevented significant photosynthesis (data not shown), which greatly reduced isoprene emissions.

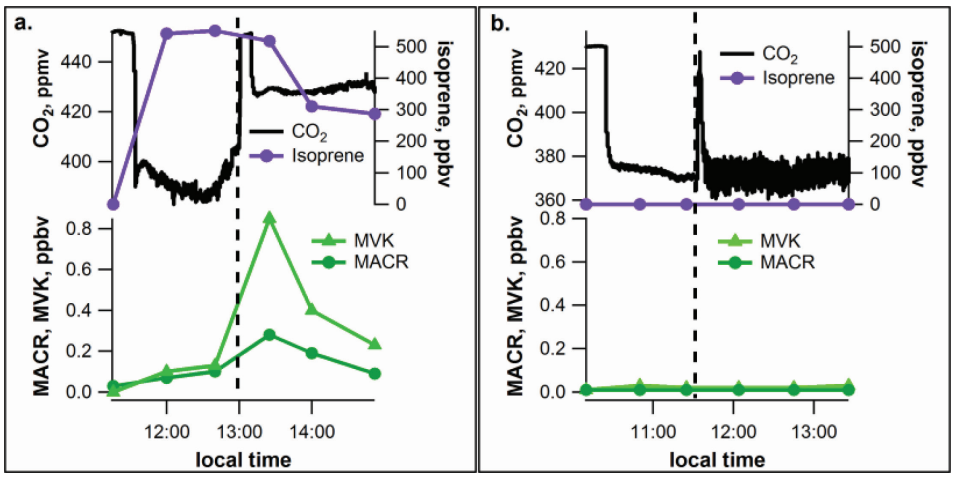

Fig. 7. Example GC-MS time series plot of MVK and MACR enclosure concentrations from mango (a) and soursop (b) following mechanical leaf wounding. The first data point is that of an empty enclosure and the vertical dashed line indicates the time that the branch was mechanically wounded (air entering enclosure measured for 10 min during this time). Also shown are the time series for CO_2 and isoprene enclosure concentrations. Note the stimulation of MVK and MACR emissions by the mechanical wounding procedure.

Monson, 1992) at high temperatures. We also showed that, under high light/temperature stress, branches emit MVK and MACR directly to the atmosphere (Jardine *et al.*, 2010*a*, 2012). We extended this analysis to include additional abiotic stresses (freeze–thaw and mechanical wounding) as well as novel putative isoprene oxidation products (MBO, 3-MF, and 3-MT) (Fig. 1). A substantial effort was made to validate the presence of these compounds in branch enclosure air and minimize the possibility of artifacts in the analytical systems. Enclosure GC-MS and PTR-MS measurements of the empty branch enclosures showed small (<0.2 ppbv) to negligible background concentrations of the compounds of interest, and GC-MS mass spectra of the compound peaks from enclosure air with mango branches matched those of the NIST mass spectral library as well as retention time and mass spectra of authentic standards. A careful calibration procedure of each analytical system with authentic standards allowed a direct comparison between enclosure concentration estimates by PTR-MS and GC-MS. During mango abiotic stress experiments, agreeable quantitative data between PTR-MS and GC-MS concentration measurements of MVK+MACR was generally found. However, PTR-MS concentration estimates for MBO, 3-MF, and 3-MT generally exceeded those determined by GC-MS, probably due to the

presence of C_5 and C_6 GLVs, which are known to be emitted from plants under stress (Fall *et al.*, 1999, 2001). Thus, the results from our study demonstrated that PTR-MS based on quadrupole mass spectrometers possess the capability to accurate quantify MVK+MACR emissions under abiotic stress, but that chromatography is needed to accurately identify and quantify 3-MF, 3-MT, and MBO. In all abiotic stress experiments, enclosure concentrations of 3-MT were very low (<0.2 ppbv). Additional research is therefore needed to verify its presence and establish its relevance to atmospheric and plant processes.

The lack of a strong enhancement in MBO, MVK, MACR, 3-MF, and 3-MT enclosure concentrations from the non-isoprene-emitting plant soursop under abiotic stress provided additional indirect evidence that isoprene oxidation within the plant cell is largely responsible for their production in mango leaves. Moreover, the rapid incorporation of photoassimilated $^{13}CO_2$ into both isoprene and the oxidized product emissions provided new evidence that these compounds derive from the direct oxidation of isoprene within mango plants. Although atmospheric oxidation of isoprene is known to produce 3-MF as a minor product (4.2–5.4%) (Atkinson and Arey, 2003), we observed 3-MF as a major emission component from high-temperature/light-stressed mango branches (Fig. 4) and freeze–thaw/desiccation (Fig. 6). On average, MACR dominated emissions of putative isoprene oxidation products from high temperature/light and freeze-thaw stress treatments of mango branches (Fig. 4). However, mechanical wounding resulted in the stimulation of higher MVK emissions than MACR (Fig. 7). The differences seen between abiotic stress factors might be attributed to different oxidation mechanisms within plants, including the generation of various ROS involved in the oxidation reactions and different downstream metabolism pathways of the various isoprene oxidation products. As ROS was not quantified in leaf tissues, the mechanism of isoprene oxidation remains speculative, as enzymatic mechanisms for isoprene oxidation remains a possibility. For example, a cytochrome P450 enzyme in mice and rats has been shown to efficiently metabolize high levels of isoprene (Bogaards *et al.*, 2001).

To date, all studies on isoprene synthase enzymes have reported only isoprene as a product (Fall and Wildermuth, 1998; Datukishvili *et al.*, 2001), while a recent in *vitro* study on MBO synthase revealed that the enzyme produces MBO to isoprene at a ratio of 90:1 (Gray *et al.*, 2011). Both isoprene and MBO are produced from the common precursor dimethylallyl diphosphate with the difference in product formation related to the exclusion (isoprene) or entry (MBO) of water into the active site of the respective synthase (Gray *et al.*, 2011). Thus, although MBO emissions from mango were shown in this study to have a similar ^{13}C-labelling pattern to that of isoprene, MBO (as well as the other oxidized compounds studied) may be produced from the oxidation of isoprene by ROS within plants or simply share the same precursor as isoprene (dimethylallyl diphosphate).

During high-temperature/light and freeze–thaw stress experiments, we generally observed two distinct patterns of putative isoprene oxidation product emissions from mango branches (e.g. Figs 4 and 5). During the first period following the initiation of stress, MBO and 3-MF emissions increased and then declined, while MACR emissions continued to increase throughout the experiment and dominated emissions near the end. If isoprene oxidation serves as the main *in vivo* source of these compounds, these observations suggest that a different isoprene oxidation mechanism occurs during early-stage versus late-stage stress. When the magnitude of the enclosure concentrations of putative isoprene oxidation products were compared between the abiotic stress treatments on mango branches, freeze–thaw/desiccation (MACR up to 17 ppbv), high light/temperature (MACR up to 4 ppbv), and mechanical wounding (MACR up to 0.4 ppbv) were ranked from highest to lowest. These observations remain consistent with the idea that freeze–thaw/desiccation may be the harshest form of abiotic stress that we applied due to the fact that most of the plant cells in the enclosed mango branch were probably damaged by this treatment. Harsh freeze–thaw stress dramatically damages membrane structures (Hincha *et al.*, 1987) and results in a massive accumulation of ROS (Heidarvand and Amiri, 2010), leading to substantial lipid peroxidation (Tajvar *et al.*, 2011). Hence, while isoprene levels were seen as relatively low after the freeze–thaw experiment, a very high pool of oxidizing species was probably available for its oxidation.

Due to high global emission rates from vegetation and rapid oxidation rates within the atmosphere, isoprene remains the most intensely investigated biogenic volatile organic compound in the Earth system. Isoprene oxidation yields a variety of first-order oxidation products including MVK, MACR, and 3-MF previously assumed to derive exclusively from atmospheric oxidation. While oxidative reactions in the atmosphere play a central role in determining air quality and climate (Monson, 2002; Pacifico *et al.*, 2009), oxidation within vegetation may protect plants from oxidative damage during stress through direct depletion of the oxidant pool and through signalling processes (Vickers *et al.*, 2009*a*). While once considered a toxic byproduct of aerobic metabolism, ROS signalling is now recognized as an integral component of plant response to abiotic and biotic stress as well as regulation of growth, development, and programmed cell death (Mittler *et al.*, 2011; Suzuki *et al.*, 2011). However, these oxidation and signalling processes remain poorly understood, in part because the quantification of ROS within plant tissues remains extremely difficult (Bournonville and Diaz-Ricci, 2011). Owing to their high reactivity and unstable nature, ROS have not been directly quantified. Instead, detection of ROS relies on quantifying products that are formed when they react with various natural or applied substances. In addition to their destructive sampling and labour-intensive nature, many existing techniques suffer from problems including the requirement to deliver cytotoxic chemicals that cause stress to tissues, poor cellular permeablility of applied chemicals, and other major artifacts (Shulaev and Oliver, 2006). As a result, the majority of methods for ROS quantification in plants are restricted to model plants (due to the presence of interferences and inhibitors) or provide only qualitative or semi-quantitative information (Shulaev and Oliver, 2006).

In this study, we configured a gas analysis system with high selectivity and sensitivity for isoprene and its putative oxidation products. The potential power of our approach may stem from the possibility that isoprene oxidation reactions leave unique volatile biomarkers behind that can be quantified in the gas phase. These volatile profiles could potentially be observed across a wide range of temporal (seconds to years) and spatial (cells to global) scales. By comparison with established techniques for determining oxidative damage in plants such as the thiobarbituric acid-reactive substances lipid peroxidation assay (Draper and Hadley, 1990), we suggest that emissions of isoprene oxidation biomarkers from plants could potentially be used as quantitative indicators of oxidative stress in plants. With changes in land use and climate change, plants are exposed to increasing levels of stress (e.g. high and low temperatures and mechanical wounding) that can result in extensive oxidative damage (Allen and Ort, 2001; Leon *et al.*, 2001; Kotak *et al.*, 2007). Development of the techniques described here may therefore help researchers understand how plants respond to oxidative stress and consequently increase our ability to predict and perhaps mitigate some of the resulting oxidative damage. Moreover, isoprene production and oxidation dynamics within plants may be important for overall forest response to climate change including expected shifts in species composition, as isoprene-producing species may be favoured as more robust responders to stresses associated with climate, air quality, and land-use changes (Harley *et al.*, 1999).

Supplementary data

Supplementary data are available at *JXB* online.

Supplementary Fig. S1. Simplified diagram of experimental setup used to identify and quantify emissions of isoprene and its putative oxidation products from mango branches using a coupled GC-MS, PTR-MS, and photosynthesis (LI-7000) system.

Acknowledgements

This research was supported by the Office of Biological and Environmental Research of the US Department of Energy under Contract no. DE-AC02-05CH11231 as part of their Terrestrial Ecosystem Science Program. Additional funding for this project came from the Philecology Foundation of Fort Worth, Texas, and instrumentation support (CHE 0216226) from the US National Science Foundation.

References

Allen DJ, Ort DR. 2001. Impacts of chilling temperatures on photosynthesis in warm-climate plants. *Trends in Plant Science* **6,** 36–42.

Allen JP, Nelson M, Alling A. 2003. The legacy of Biosphere 2 for the study of biospherics and closed ecological systems. *Space Life Sciences: Closed Artificial Ecosystems and Life Support Systems* **31,** 1629–1639.

Almeras E, Stolz S, Vollenweider S, Reymond P, Mene-Saffrane L, Farmer EE. 2003. Reactive electrophile species activate defense gene expression in *Arabidopsis*. *The Plant Journal* **34,** 202–216.

Atkinson R, Arey J. 2003. Gas-phase tropospheric chemistry of biogenic volatile organic compounds: a review. *Atmospheric Environment* **37,** S197-S219.

Bogaards JJP, Freidig AP, van Bladeren PJ. 2001. Prediction of isoprene diepoxide levels in vivo in mouse, rat and man using enzyme kinetic data in vitro and physiologically-based pharmacokinetic modelling. *Chemico-Biological Interactions* **138,** 247–265.

Bournonville CFG, Diaz-Ricci JC. 2011. Quantitative determination of superoxide in plant leaves using a modified NBT staining method. *Phytochemical Analysis* **22,** 268–271.

Datukishvili NT, Tarkhnishvili GM, Mikeladze DG, Beridze TG, Sanadze GA. 2001. Isolation and purification of protein responsible for the conversion of dimethylallylpyrophosphate from poplar leaves into isoprene. *Russian Journal of Plant Physiology* **48,** 222–225.

Draper HH, Hadley M. 1990. Malondialdehyde determination as index of lipid-peroxidation. *Methods in Enzymology* **186,** 421–431.

Engelhart GJ, Moore RH, Nenes A, Pandis SN. 2011. Cloud condensation nuclei activity of isoprene secondary organic aerosol. *Journal of Geophysical Research: Atmospheres* **116,** D02207.

Fall R, Karl T, Hansel A, Jordan A, Lindinger W. 1999. Volatile organic compounds emitted after leaf wounding: on-line analysis by proton-transfer-reaction mass spectrometry. *Journal of Geophysical Research: Atmospheres* **104,** 15963–15974.

Fall R, Karl T, Jordon A, Lindinger W. 2001. Biogenic C5 VOCs: release from leaves after freeze-thaw wounding and occurrence in air at a high mountain observatory. *Atmospheric Environment* **35,** 3905–3916.

Fall R, Monson RK. 1992. Isoprene emission rate and intercellular isoprene concentration as influenced by stomatal distribution and conductance. *Plant Physiology* **100,** 987–992.

Fall R, Wildermuth MC. 1998. Isoprene synthase: from biochemical mechanism to emission algorithm. *Journal of Geophysical Research: Atmospheres* **103,** 25599–25609.

Farmer EE, Davoine C. 2007. Reactive electrophile species. *Current Opinion in Plant Biology* **10,** 380–386.

Feher A, Otvos K, Pasternak TP, Szandtner AP. 2008. The involvement of reactive oxygen species (ROS) in the cell cycle activation (G_0-to-G_1 transition) of plant cells. *Plant Signaling & Behavior* **3,** 823–826.

Foreman J, Demidchik V, Bothwell JHF, *et al.* 2003. Reactive oxygen species produced by NADPH oxidase regulate plant cell growth. *Nature* **422,** 442–446.

Funk JL, Mak JE, Lerdau MT. 2004. Stress-induced changes in carbon sources for isoprene production in *Populus deltoides*. *Plant Cell and Environment* **27,** 747–755.

Gray DW, Breneman SR, Topper LA, Sharkey TD. 2011. Biochemical characterization and homology modeling of methylbutenol synthase and implications for understanding hemiterpene synthase evolution in plants. *Journal of Biological Chemistry* **286,** 20582–20590.

Guenther A, Karl T, Harley P, Wiedinmyer C, Palmer PI, Geron C. 2006. Estimates of global terrestrial isoprene emissions using MEGAN (Model of Emissions of Gases and Aerosols from Nature). *Atmospheric Chemistry and Physics* **6,** 3181–3210.

Harley P, Vasconcellos P, Vierling L, *et al.* 2004. Variation in potential for isoprene emissions among Neotropical forest sites. *Global Change Biology* **10,** 630–650.

Harley PC, Monson RK, Lerdau MT. 1999. Ecological and evolutionary aspects of isoprene emission from plants. *Oecologia* **118,** 109–123.

Heidarvand L, Amiri RM. 2010. What happens in plant molecular responses to cold stress? *Acta Physiologiae Plantarum* **32,** 419–431.

Hincha DK, Hofner R, Schwab KB, Heber U, Schmitt JM. 1987. Membrane rupture is the common cause of damage to chloroplast membranes in leaves injured by freezing or excessive wilting. *Plant Physiology* **83,** 251–253.

Jardine K, Abrell L, Jardine A, Huxman T, Saleska S, Arneth A, Monson R, Karl T, Fares S, Loreto F, Goldstein A. 2012. Within-plant isoprene oxidation confirmed by direct emissions of oxidation products methyl vinyl ketone and methacrolein. *Global Change Biololgy* **18,** 973–984.

Jardine K, Abrell L, Kurc SA, Huxman T, Ortega J, Guenther A. 2010*a*. Volatile organic compound emissions from *Larrea tridentata* (creosotebush). *Atmospheric Chemistry and Physics* **10,** 12191–12206.

Jardine K, Sommer E, Saleska S, Huxman T, Harley P, Abrell L. 2010*b*. gas phase measurements of pyruvic acid and its volatile metabolites. *Environmental Science & Technology* **44,** 2454–2460.

Jardine KJ, Henderson WM, Huxman TE, Abrell L. 2010*c*. Dynamic solution injection: a new method for preparing pptv–ppbv standard atmospheres of volatile organic compounds. *Atmospheric Measurement Techniques* **3,** 1569–1576.

Karl T, Fall R, Rosenstiel TN, Prazeller P, Larsen B, Seufert G, Lindinger W. 2002. On-line analysis of the $^{13}CO_2$ labeling of leaf isoprene suggests multiple subcellular origins of isoprene precursors. *Planta* **215,** 894–905.

Karl T, Harley P, Emmons L, Thornton B, Guenther A, Basu C, Turnipseed A, Jardine K. 2010. Efficient atmospheric cleansing of oxidized organic trace gases by vegetation. *Science* **330,** 816–819.

Keller M, Lerdau M. 1999. Isoprene emission from tropical forest canopy leaves. *Global Biogeochemical Cycles* **13,** 19–29.

Kotak S, Larkindale J, Lee U, von Koskull-Doring P, Vierling E, Scharf KD. 2007. Complexity of the heat stress response in plants. *Current Opinion in Plant Biology* **10,** 310–316.

Kroll JH, Ng NL, Murphy SM, Flagan RC, Seinfeld JH. 2006. Secondary organic aerosol formation from isoprene photooxidation. *Environmental Science & Technology* **40,** 1869–1877.

Kwak JM, Mori IC, Pei ZM, Leonhardt N, Torres MA, Dangl JL, Bloom RE, Bodde S, Jones JDG, Schroeder JI. 2003. NADPH oxidase *AtrbohD* and *AtrbohF* genes function in ROS-dependent ABA signaling in *Arabidopsis*. *EMBO Journal* **22,** 2623–2633.

Leon J, Rojo E, Sanchez-Serrano JJ. 2001. Wound signalling in plants. *Journal of Experimental Botany* **52,** 1–9.

Lindinger W, Hansel A. 1997. Analysis of trace gases at ppb levels by proton transfer reaction mass spectrometry (PTR-MS). *Plasma Sources Science & Technology* **6,** 111–117.

Lockwood AL, Shepson PB, Fiddler MN, Alaghmand M. 2010. Isoprene nitrates: preparation, separation, identification, yields, and atmospheric chemistry. *Atmospheric Chemistry and Physics* **10,** 6169–6178.

Loreto F, Delfine S. 2000. Emission of isoprene from salt-stressed *Eucalyptus globulus* leaves. *Plant Physiology* **123,** 1605–1610.

Loreto F, Mannozzi M, Maris C, Nascetti P, Ferranti F, Pasqualini S. 2001. Ozone quenching properties of isoprene and its antioxidant role in leaves. *Plant Physiology* **126,** 993–1000.

Loreto F, Velikova V. 2001. Isoprene produced by leaves protects the photosynthetic apparatus against ozone damage, quenches ozone products, and reduces lipid peroxidation of cellular membranes. *Plant Physiol* . **127,** 1781–1787.

Miller G, Suzuki N, Ciftci-Yilmaz S, Mittler R. 2010. Reactive oxygen species homeostasis and signalling during drought and salinity stresses. *Plant Cell and Environment* **33,** 453–467.

Mittler R, Vanderauwera S, Suzuki N, Miller G, Tognetti VB, Vandepoele K, Gollery M, Shulaev V, Van Breusegem F. 2011. ROS signaling: the new wave? *Trends in Plant Science* **16,** 300–309.

Mittler R. 2002. Oxidative stress, antioxidants and stress tolerance. *Trends in Plant Science* **7,** 405–410.

Monson RK. 2002. Volatile organic compound emissions from terrestrial ecosystems: a primary biological control over atmospheric chemistry. *Israel Journal of Chemistry* **42,** 29–42.

Mullineaux P, Karpinski S. 2002. Signal transduction in response to excess light: getting out of the chloroplast. *Current Opinion in Plant Biology* **5,** 43–48.

Overmyer K, Brosche M, Kangasjarvi J. 2003. Reactive oxygen species and hormonal control of cell death. *Trends in Plant Science* **8,** 335–342.

Pacifico F, Harrison SP, Jones CD, Sitch S. 2009. Isoprene emissions and climate. *Atmospheric Environment* **43,** 6121–6135.

Pei ZM, Murata Y, Benning G, Thomine S, Klusener B, Allen GJ, Grill E, Schroeder JI. 2000. Calcium channels activated by hydrogen peroxide mediate abscisic acid signalling in guard cells. *Nature* **406,** 731–734.

Pierce T, Geron C, Bender L, Dennis R, Tonnesen G, Guenther A. 1998. Influence of increased isoprene emissions on regional ozone modeling. *Journal of Geophysical Research: Atmospheres* **103,** 25611–25629.

Shulaev V, Oliver DJ. 2006. Metabolic and proteomic markers for oxidative stress. New tools for reactive oxygen species research. *Plant Physiology* **141,** 367–372.

Singsaas EL, Lerdau M, Winter K, Sharkey TD. 1997. Isoprene increases thermotolerance of isoprene-emitting species. *Plant Physiology* **115,** 1413–1420.

Suzuki N, Miller G, Morales J, Shulaev V, Torres MA, Mittler R. 2011. Respiratory burst oxidases: the engines of ROS signaling. *Current Opinion in Plant Biology* **14,** 691–699.

Tajvar Y, Ghazvini RF, Hamidoghli Y, Sajedi RH. 2011. Antioxidant changes of Thomson navel orange (*Citrus sinensis*) on three rootstocks under low temperature stress. *Horticulture Environment and Biotechnology* **52,** 576–580.

Uchida K, Kanematsu M, Morimitsu Y, Osawa T, Noguchi N, Niki E. 1998. Acrolein is a product of lipid peroxidation reaction. Formation of free acrolein and its conjugate with lysine residues in oxidized low density lipoproteins. *Journal of Biological Chemistry* **273,** 16058–16066.

Velikova V, Edreva A, Loreto F. 2004. Endogenous isoprene protects *Phragmites australis* leaves against singlet oxygen. *Physiol. Plantarum* **122,** 219–225.

Velikova V, Sharkey T, Loreto F. 2012. Stabilization of thylakoid membranes in isoprene-emitting plants reduces formation of reactive oxygen species. *Plant Signal Behavior* **7,** 139–141.

Velikova V, Varkonyi Z, Szabo M, *et al.* 2011. Increased thermostability of thylakoid membranes in isoprene-emitting leaves probed with three biophysical techniques. *Plant Physiology* **157,** 905–916.

Vickers CE, Gershenzon J, Lerdau MT, Loreto F. 2009*a*. A unified mechanism of action for volatile isoprenoids in plant abiotic stress. *Nature Chemical Biology* **5,** 283–291.

Vickers CE, Possell M, Cojocariu CI, Velikova VB, Laothawornkitkul J, Ryan A, Mullineaux PM, Hewitt CN. 2009*b*. Isoprene synthesis protects transgenic tobacco plants from oxidative stress. *Plant Cell and Environment* **32,** 520–531.

Vickers CE, Possell M, Laothawornkitkul J, Ryan AC, Hewitt CN, Mullineaux PM. 2011. Isoprene synthesis in plants: lessons from a transgenic tobacco model. *Plant Cell and Environment* **34,** 1043–1053.